Neuro-Oncology

Neuro-Oncology 17(9), 1210–1219, 2015
doi:10.1093/neuonc/nov081
Advance Access date 12 May 2015

Decreased affinity for efflux transporters increases brain penetrance and molecular targeting of a PI3K/mTOR inhibitor in a mouse model of glioblastoma

Chani M. Becker†, Rajneet K. Oberoi†, Stephan J. McFarren, Daniel M. Muldoon, Deanna H. Pafundi, Jenny L. Pokorny, Debra H. Brinkmann, John R. Ohlfest‡, Jann N. Sarkaria, David A. Largaespada, and William F. Elmquist

Department of Neuroscience, University of Minnesota, Minneapolis, Minnesota (C.M.B., S.J.M., D.M.M., J.R.O., W.F.E); Brain Tumor Program, University of Minnesota, Minneapolis, Minnesota (C.M.B., R.K.O., S.J.M., D.M.M., J.R.O., D.A.L., W.F.E); Department of Pharmaceutics, University of Minnesota, Minneapolis, Minnesota (R.K.O., W.F.E); Department of Pediatrics, University of Minnesota, Minneapolis, Minnesota (J.R.O., D.A.L); Department of Radiation Oncology, Mayo Clinic, Rochester, Minnesota (D.H.P., J.L.P., D.H.B., J.N.S); Brain Barriers Research Center, University of Minnesota, Minneapolis, Minnesota

Corresponding Author: William F. Elmquist, PhD, Department of Pharmaceutics, University of Minnesota, 9-177 Weaver-Densford Hall, 308 Harvard Street SE, Minneapolis, MN 55455 (elmqu011@umn.edu).

†C.M.B. and R.K.O. contributed equally to this work and share first authorship.

‡Author is deceased.

See the editorial by Mason, on pages 1181–1182.

Background. Targeting drug delivery to invasive glioma cells is a particularly difficult challenge because these cells lie behind an intact blood-brain barrier (BBB) that can be observed using multimodality imaging. BBB-associated efflux transporters such as P-glycoprotein (P-gp) and breast cancer resistance protein (BCRP) influence drug distribution to these cells and may negatively impact efficacy. To test the hypothesis that efflux transporters influence brain pharmacokinetics/pharmacodynamics of molecularly targeted agents in glioma treatment, we assessed region-specific penetrance and molecular-targeting capacity for a PI3K/mTOR kinase inhibitor that has high substrate affinity for efflux transporters (GDC-0980) and an analog (GNE-317) that was purposely designed to have reduced efflux.

Methods. Brain tumor penetrance of GDC-0980 and GNE-317 was compared between FVB/n wild-type mice and *Mdr1a/b*$^{-/-}$*Bcrp*$^{-/-}$ triple-knockout mice lacking P-gp and BCRP. C57B6/J mice bearing intracranial GL261 tumors were treated with GDC-0980, GNE-317, or vehicle to assess the targeted pharmacokinetic/pharmacodynamic effects in a glioblastoma model.

Results. Animals treated with GNE-317 demonstrated 3-fold greater penetrance in tumor core, rim, and normal brain compared with animals dosed with GDC-0980. Increased brain penetrance correlated with decreased staining of activated p-Akt, p-S6, and p-4EBP1 effector proteins downstream of PI3K and mTOR.

Conclusions. GDC-0980 is subject to active efflux by P-gp and BCRP at the BBB, while brain penetrance of GNE-317 is independent of efflux, which translates into enhanced inhibition of PI3K/mTOR signaling. These data show that BBB efflux by P-gp and BCRP is therefore an important determinant in both brain penetrance and molecular targeting efficacy in the treatment of invasive glioma cells.

Keywords: blood-brain barrier, brain tumors, efflux transport, molecularly targeted agents, p-glycoprotein.

Glioblastoma (GBM) is the most commonly diagnosed primary tumor of the central nervous system, with 20 000 new cases diagnosed annually in the United States. Median survival for patients diagnosed with GBM is only 14 months and has not improved in recent years despite major advances in molecularly targeted chemotherapies.[1] Knowledge of the genetic and molecular mechanisms driving GBM and other types of cancers has led to the creation of targeted kinase inhibitors; despite

Received 3 December 2014; accepted 8 April 2015

such specific targeting, however, such drugs have not been clinically successful. These failures in clinical trials are often attributed to ineffective drugs, poor target selection, or various molecular mechanisms of resistance.[2,3] Unfortunately, there has been limited consideration of drug delivery in the treatment of GBM and the inability of these drugs to effectively reach their targets.

Delivery of chemotherapeutics to the brain remains a significant challenge in the treatment of GBM because of the tumor's invasive nature. Advanced imaging techniques demonstrate the presence of invasive cells that are protected by an intact blood-brain barrier (BBB) and therefore remain largely inaccessible to chemotherapeutics (Fig. 1). These imaging modalities that show changes in the BBB and extent of tumor invasiveness have been previously described.[4] T1-gadolinium contrast-enhanced (T1-CE) MR is limited in detecting only the core tumor mass where the BBB is disrupted[5] and cannot detect invasive glioma cells in surrounding areas where the BBB remains intact (middle panels, Fig. 1A and B). Alternatively, ^{18}F-DOPA PET (right panels, Fig. 1A and B) and T2-weighted fluid-attenuated inversion recovery MR scans (left panels, Fig. 1A and B) delineate a larger volume of tumor than T1-CE in the same patients (quantified signal volumes in Supplementary material, Fig. S1). Because glioma detection and the extent of malignant regions for surgical resection are primarily determined through contrast enhancement on T1-CE,[4] some portion of the tumor is invariably left behind during surgery (Fig. 1B). These images from glioma patients clearly demonstrate the need for chemotherapeutics capable of accessing invasive glioma cell populations that lie behind the protection of an intact BBB. Effective drug delivery to these invasive glioma cells is therefore a crucial objective in chemotherapeutic design, and the BBB is an important impediment to this goal.[6] Endothelial-cell tight junctions form a physical barrier that limits the influx of xenobiotics into the brain, while a biochemical barrier formed by transporters like P-gp and BCRP[7] effectively effluxes substrate molecules.[8,9] Intelligent drug design must address both components of the BBB to ensure successful delivery of a chemotherapeutic. Pharmacological inhibition of efflux transporters has been tested against systemic tumors with minimal clinical gains in efficacy;[10,11] however, neither pharmacological inhibition of efflux nor improved drug design has been specifically employed to improve CNS drug delivery, especially to invasive glioma. Therefore, an important approach to improving chemotherapeutic brain penetrance would be to develop novel therapeutics that do not have efflux transporter liabilities but do have adequate intrinsic permeability- penetrant chemotherapeutics has traditionally addressed several key molecular characteristics including size, charge, lipophilicity, polarity, and molecular flexibility.[12,13] However, the affinity for drug efflux

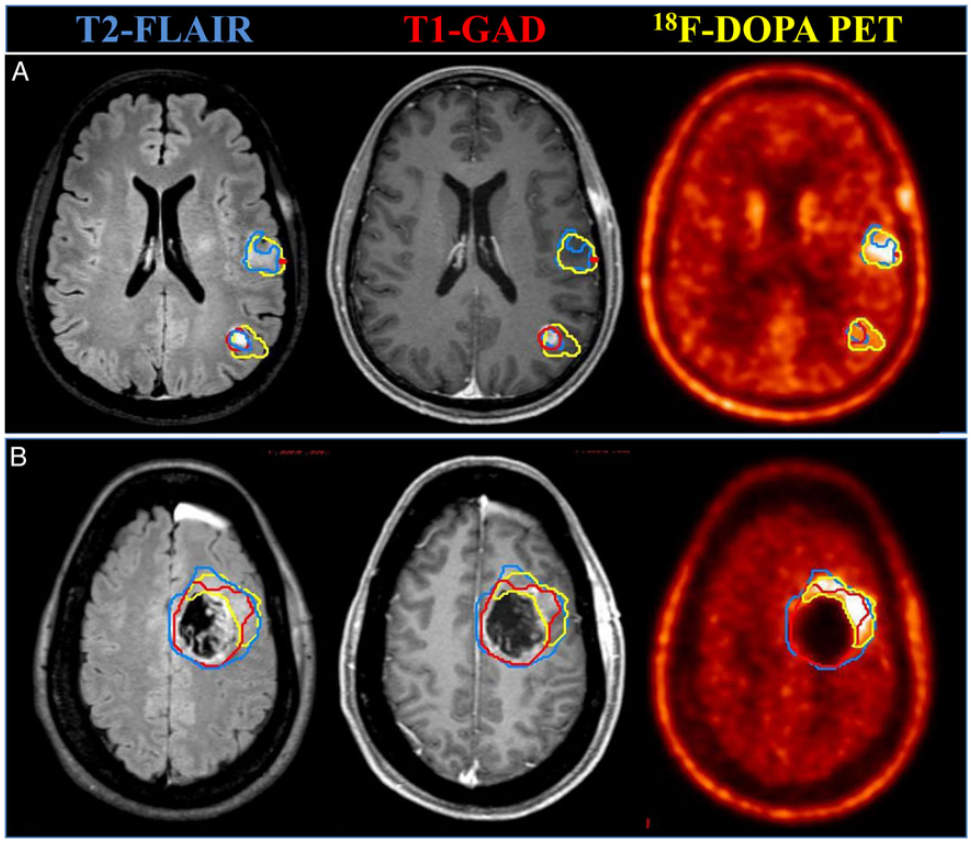

Fig. 1. Different imaging modalities visualize tumors residing behind an intact blood-brain barrier. (A) Patient exhibiting multifocal glioblastoma with large tumors displayed through ^{18}F-DOPA PET imaging. (B) Another patient 3 weeks post surgical resection exhibits obvious tumor via ^{18}F-DOPA PET that was missed during surgery.

transporters is rarely considered despite recent advances in computational modeling that predict (with 90% accuracy) a molecule's efflux pump substrate affinity from its molecular structure.[14] This recent work has led to identification of pharmacophores specific to substrates and nonsubstrates. Examples include amines and aromatic rings for "effluxophores" and aliphatic rings or saturated aliphatic chains for "anti-effluxophores."[14] These features should serve to guide future development of brain-penetrant chemotherapeutics.

The purposes of this study were to compare 2 dual PI3K/mTOR inhibitors with different affinities for P-gp and BCRP with respect to their BBB penetration to specific regions of tumor and to determine how these tumor-delivery differences translate to molecular targeting efficacy and survival. An understanding of this mechanism in different regions of the brain tumor will allow us to develop compounds and novel therapeutics that can be more effective against invasive GBM (ie, those tumor cells that are left behind following resection).[15] We hypothesized that the strategic re-design of GDC-0980, a compound with high affinity for the described BBB efflux pumps, into a low-affinity oxetane derivative GNE-317[16] would mediate not only increased brain penetrance but also a greater ability to inhibit PI3K/mTOR pathways and improve survival in the GL261 model. Inhibition of these targets in particular is an important clinical goal because these pathways drive GBM growth and development.[17,18] In our work, we characterized the differential pharmacokinetic and pharmacodynamic properties of these compounds in vivo. Our data show that decreasing the substrate affinity for P-gp and BCRP increases brain penetrance and improves inhibition of the targeted signaling pathways. Collectively, these data suggest that brain-penetrant molecularly targeted anticancer agents may be more efficacious in glioma if they demonstrate minimal substrate affinity for BBB efflux transporters and that the targeted agents are appropriate for the genetic drivers of tumor growth. Furthermore, the advent of such drugs may be derived from existing compounds rather than being synthesized de novo.

Materials and Methods

Animal Care

All procedures were carried out in accordance with the guidelines set by the Principles of Laboratory Animal Care (National Institutes of Health, Bethesda, Maryland) and were approved by the Institutional Animal Care and Use Committee (IACUC) of the University of Minnesota. Animals were allowed food and water ad libitum. Female C57BL/6J mice were purchased from Jackson Laboratory. FVB/n wild-type (WT), *Mdr1a/b*−/− (P-gp knockout [PKO] mice), *Bcrp*−/− (BCRP knockout [BKO] mice), and *Mdr1a/b*$^{-/-}$*Bcrp*$^{-/-}$ mice (triple knockout [TKO] mice) were all purchased from Taconic Farms Inc.

Chemicals and Reagents

GDC-0980 and GNE-317 were provided by Genentech Inc. Drugs were suspended in dimethylsulfoxide (DMSO) for in vitro studies and in a vehicle of 0.5% methyl cellulose with 0.2% Tween 80 for in vivo work. Ammonium formate and acetonitrile were high-performance liquid chromatography (HPLC) grade and were procured from Sigma-Aldrich. Texas Red dextran (TRD) 3000 MW was purchased from Molecular Probes (Invitrogen).

Tissue Culture

GL261 is an aggressive C57BL/6J-derived glioma line.[19] This cell line was a kind gift from Dr. John Ohlfest (University of Minnesota) and was transfected with both green fluorescent protein (GFP) and luciferase (Luc) from separate plasmids using methods described previously.[20] The resultant monoclonal GL261-GFP-Luc cells were maintained in Dulbecco's modified Eagle's medium supplemented with 10% FBS and penicillin/streptomycin (100 U/mL) and cultured at 5% oxygen. Cell selection used 4 mg/mL puromycin (InvivoGen) and 4 mg/mL G418 (InvivoGen). Cellular viability assays were set up in a 96-well format with 2000 cells plated per well in the culture conditions described previously. Cells were incubated in the presence of drug or vehicle for 48 hours, and viability was assessed by 3-(4,5-dimethylthiazol-2-yl)-5-(3-carboxymethoxyphenyl)-2-(4-sulfophenyl)-2H-tetrazolium (MTS) assay (Promega) according to the manufacturer's instructions. Absorbance at 490 nm was used to determine viability and at 650 nm to account for background using a Synergy Mx automated plate reader (BioTek). Numerical values from drug-treated wells were normalized to the values of vehicle-treated wells to yield percent survival.

Intracranial Tumor Implantation

Gliomas were established by intracranial inoculation of 30 000 GL261-GFP-Luc cells in 1 μL volume to 7-week-old C57BL/6J mice as previously described.[21] Cells were prepared for inoculation by culturing to subconfluence and washing with phosphate-buffered saline (PBS), followed by trypsinization and filtration through a 40 μm mesh and resuspension in sterile PBS. Animals were anesthetized with an i.p. injection of a ketamine/xylazine cocktail (53.7 mg/mL and 9.26 mg/mL xylazine delivered 1 mL/kg) before surgery. Cells were injected into the right ventral striatum at coordinates 2.5 mm lateral and 0.5 mm anterior from the bregma at a ventral depth of 3 mm from the surface of the brain.[21] Cells were injected at a continuous rate of 0.2 μL per minute over 5 minutes. The progression of tumor growth was determined through bioluminescence imaging using the IVIS50 system (Caliper Life Sciences) after a 100 μL i.p. injection of 28.5 mg/mL d-luciferin (substrate for luciferase enzyme; Gold Biotechnology) 10 minutes before imaging.[22] Animals were sedated using 2%–5% isoflurane provided by nose cones within the imager. In survival studies, mice that became moribund were euthanized with carbon dioxide.

Blood-brain Barrier Imaging

When tumors reached a signal of 5e8 p/s/cm2/sr, C57BL/6J mice bearing GL261-GFP-Luc tumors were given an i.v. injection of 1.5 mg/mL TRD (3000 MW).[23] After 10 minutes, animals were euthanized with carbon dioxide and perfused with 10 mL PBS over 1 minute. Brains were harvested and flash frozen in isopentane (−80°C). Brains were sliced on a cryostat into 20 μm sections and mounted on charged glass slides. Sections were imaged using the GFP and Texas Red filters of a Leica DMI 6000B microscope. Images were acquired in grayscale using an

associated Retiga 2000R camera (QImaging) at a variety of exposure times; the different exposure times were necessary to increase visualization in the smaller tumor-bearing slices and to prevent signal saturation in the larger tumor-bearing slices. The individual images were acquired using QImaging QCapture Pro v 6.0 software, compiled (Microsoft Image Composite Editor), and synthetically colored (Adobe Photoshop).

Steady-state Pharmacokinetics

The steady-state brain-to-plasma ratios for both GDC-0980 and GNE-317 were determined using Alzet osmotic minipumps (model 1003D; Durect Corporation) in FVB/n mice. The minipumps were filled with 100 μL of either a 5 mg/mL solution in DMSO of GNE-317 or a 10 mg/mL solution in DMSO of GDC-0980. On the day of the experiment, mice were anesthetized using 5% isoflurane and maintained under anesthesia with 2% isoflurane during surgery. The pumps were surgically implanted into the peritoneal cavity of the mice, after which the mice were allowed to recover on a heated pad. The pumps yielded a constant i.p. infusion of 5 μg GNE-317/hour or 10 μg GDC-0980/hour. For GDC-0980, additional steady-state analyses were carried out in PKO, BKO, and TKO mice. After 48 hours (>5 half-lives for either drug), animals were euthanized, and both blood and brain were harvested and processed as described previously.[24] Briefly, whole brains were rapidly removed, rinsed with ice-cold saline, blotted dry, and transferred to preweighed tubes. Plasma was obtained by centrifuging the blood at 3500 rpm for 15 minutes at 4°C. Plasma and brain specimens were stored at −80°C until analysis by HPLC-tandem mass spectrometry (HPLC-MS/MS).

Quantification of GNE-317 and GDC-0980 in Brain and Plasma by LC-MS/MS

The plasma and brain concentrations of GNE-317 and GDC-0980 were determined using HPLC-MS/MS. On the day of the analysis, frozen brain samples were thawed at room temperature, and brain weights were determined. Samples were homogenized using 3 volumes of 5% ice-cold bovine serum albumin prepared in PBS (pH = 7.4). Brain concentrations were corrected for the residual drug in brain vascular space.[25] Drug concentrations in GNE-317 alone or GDC-0980 alone treated groups were analyzed as follows: 100 μL of plasma or 200 μL of brain homogenate samples were placed in microcentrifuge tubes containing 10 μL of 2 μg/mL internal standard (GNE-317: AG1478 [4-{3-chloroanilino}-6,7-dimethoxyquinazoline] or GDC-0980: dasatinib, free base) and extracted via vigorous vortexing with 500 μL of ice-cold ethyl acetate. Following centrifugation at 7500 rpm for 15 minutes at 4°C, 400 μL of the supernatant were transferred to microcentrifuge tubes and dried under nitrogen. Dried samples were reconstituted with 100 μL of mobile phase for GNE-317 (60:40:0.1, v/v%, 20 mM ammonium formate, pH 3.5: acetonitrile: formic acid) or GDC-0980 (72:28:0.1, v/v/v%, 20 mM ammonium formate, pH 3.5: acetonitrile: formic acid) and transferred to glass autosampler vials. The chromatographic system consisted of Agilent Technologies model 1200 HPLC system. Separation of the analyte was achieved using Agilent ZORBAX XDB Eclipse C_{18} column (4.6 × 50 mm, 1.8 μm). The LC-system was linked to TSQ Quantum triple quadrupole mass spectrometer (Thermo Finnigan), and data analysis was performed using Xcalibur software. The instrument was equipped with selected reaction monitoring mode with an electrospray ionization source operated in positive ion mode at a spray voltage of 5000V for both GNE-317 and GDC-0980. The mobile phase flow rate was 0.25 mL/min. The mass-to-charge transitions were programmed for GNE-317 (415.11→385.13) and internal standard AG1478, (317.03→300.98) and GDC-0980 (499.24→340.98) and internal standard dasatinib (499→401). The assays were both linear over a range of 1.9 ng/mL to 1000 ng/mL with a coefficient of variation lower that 20% for all samples throughout both assays.

Regional Distribution of GDC-0980 and GNE-317 in GL261 Tumor-bearing Mice

GL261-GFP-Luc cells were implanted into 7-week-old C57BL/6J mice. When tumors reached 5e7 photons/s/cm^2/sr (radiance), animals were orally administered the maximum tolerated dose of GDC-0980 (7.5 mg/kg), GNE-317 (30 mg/kg) or vehicle once a day for 3 days. The maximum tolerated doses were defined as the greatest dose that could be administered to mice with <10% drop in bodyweight. Even at these different doses, both doses provided similar plasma concentrations and thus the same overall systemic exposure. At 1 or 6 hours after the third dose, mice were euthanized with carbon dioxide and perfused with 30 mL PBS. With the aid of GFP goggles (Biological Laboratory Equipment), brains were dissected into tumor core, tumor rim, and normal brain tissue.[23] Tissue samples and blood were processed as described previously, and tissue specimens from each group were analyzed for drug concentrations using LC-MS/MS.

Immunohistochemistry

GL261-GFP-Luc cells were implanted into 7-week-old C57BL/6J mice. When tumors reached bioluminescence radiance of 5e7 p/s/cm^2/sr, mice were randomized into 3 groups ($n = 5–6$ animals/group): (i) control (vehicle treated, p.o.), (ii) GDC-0980 (7.5 mg/kg, p.o.), and (iii) GNE-317 (30 mg/kg, p.o.). Drug solutions were prepared and administered once per day for 3 days as described previously. All mice were euthanized with carbon dioxide 1 or 6 hours after the third dose and perfused with 30 mL PBS. Brains were harvested and stored in 10% buffered formalin for 24 hours and then switched to 70% ethanol until processing. Formalin-fixed, paraffin-embedded brains were sectioned at 5 μm thickness and then heat-fixed onto charged glass slides for staining. Following deparaffinization and rehydration, antigen epitopes on tissue sections were exposed using an unmasking solution (Vector Laboratories). Tissue section slides were then exposed to 3% hydrogen peroxide to remove endogenous peroxidases. Blocking was conducted with 3% bovine serum albumin (BSA) in a humidified chamber overnight at 4°C. Sections were then treated with primary antibody (Akt, 1:200; p-Akt^{Ser473}, 1:50; 4EBP1, 1: 1000; p-4EBP1$^{Thr37/46}$, 1:1000; S6, 1:100; p-S6$^{Ser235/236}$, 1:50 [all from Cell Signaling]) in 1% BSA and allowed to incubate overnight at 4°C in a humidified chamber. After primary incubation, sections were PBS-washed before incubating with 1:200 biotinylated goat

anti-rabbit secondary antibody (Vector Laboratories) for 1 hour at room temperature. Sections were washed twice in PBS before a 30-minute application of an avidin/biotinylated enzyme complex conjugated to horseradish peroxidase (Vectastain Elite ABC kit, Vector Laboratories). After 2 washes in PBS, the sections were treated with freshly prepared 3,3′-diaminobenzidine substrate prepared according to the manufacturer's instructions (Vector Laboratories) and allowed to develop. Once a discernible signal was obtained, the reaction was stopped by placing slides in water. Finally, sections were counterstained with hematoxylin, dehydrated, cleared in xylenes, and mounted in Permount (Fisher Scientific). Images were acquired in color with a Nikon AZ100 Macrofluorescence microscope. NIS-Elements software (Nikon Instruments, Inc.) was used to automatically stitch individual pictures.

Statistical Analysis

The unpaired 2-sample *t* test was used to compare between 2 groups. One-way ANOVA, followed by Bonferroni's test, was conducted to test for significance among multiple groups. Significance was declared at $P < .05$ for all tests. All tests were done using GraphPad Prism 5.01. Survival probabilities were estimated using Kaplan-Meier survival curves, and the treatment groups were compared using the log-rank test.

Results

The GL261 Glioma Model Is Characterized by Heterogeneous Blood-brain Barrier Disruption

Invasiveness of the GL261 model has already been established[19] and is even present on a macroscopic scale (Fig. 2A). BBB disruption has been assessed in this model using T1-CE MRI,[26] but microscopic dye-based permeability studies provide a higher spatial resolution of these patterns of BBB disruption. In humans, BBB disruption is not homogeneous within the central tumor mass (see Fig. 1, middle panel); rather, the tumor core displays heterogeneous disruption while the tumor rim (ie, the invasive edge) demonstrates an intact BBB.[6] To determine whether the GL261 model displays comparable deficits, a 3 kDa TRD permeability marker was injected into mice intravenously and allowed to circulate for 10 minutes. Penetrance of the dye was assessed in proximity to the GFP-positive tumor cells using fluorescence microscopy. Analysis reveals that at all tumor sizes, TRD accumulates heterogeneously at the center of the tumor mass with little to no accumulation at the tumor rim (Fig. 2B and C). This animal model therefore recapitulates the patterns of BBB disruption seen in human GBM.

GNE-317 Exhibits Similar Cytotoxic Activity and Greater Brain Penetrance Than GDC-0980

GNE-317 is an oxetane derivative of GDC-0980 synthesized with the goal of reducing substrate affinity for efflux transporters.[16] Despite the molecular changes at the piperizine group, both compounds retained the same molecular backbone including the Morpholino and 2-aminopyrimidyl groups (Fig. 3A). In vitro, GDC-0980 and GNE-317 demonstrated similar profiles in MTS cytotoxicity experiments using the GL261 cell line. These results suggest that the retained molecular structure common to both drugs allows for similar interactions with PI3K and mTOR targets (Fig. 3B). The steady-state distribution of each drug to the brain was determined in mice implanted with mini-osmotic pumps that provided a continuous intraperitoneal infusion of either GDC-0980 or GNE-317. Both WT and TKO (*Mdr1/b*$^{-/-}$ *Bcrp*$^{-/-}$) mice were used to ascertain the influence of P-gp and BCRP on the transport of drug across the BBB (Supplementary material, Fig. S2). After 48 hours of drug exposure, blood and brains were harvested and analyzed via LC-MS/MS. In animals dosed with GDC-0980, the steady-state brain-to-plasma ratio was 0.1 ± 0.02 in WT mice and 1.03 ± 0.27 in TKO mice, a 10-fold increase in brain distribution when both P-gp and BCRP were absent (Fig. 3C). In contrast, the brain-to-plasma ratios in animals dosed with GNE-317 were similar between WT and TKO mice (0.81 ± 0.28 vs 0.98 ± 0.78) (Fig. 3D). Collectively, these data indicate that P-gp and BCRP

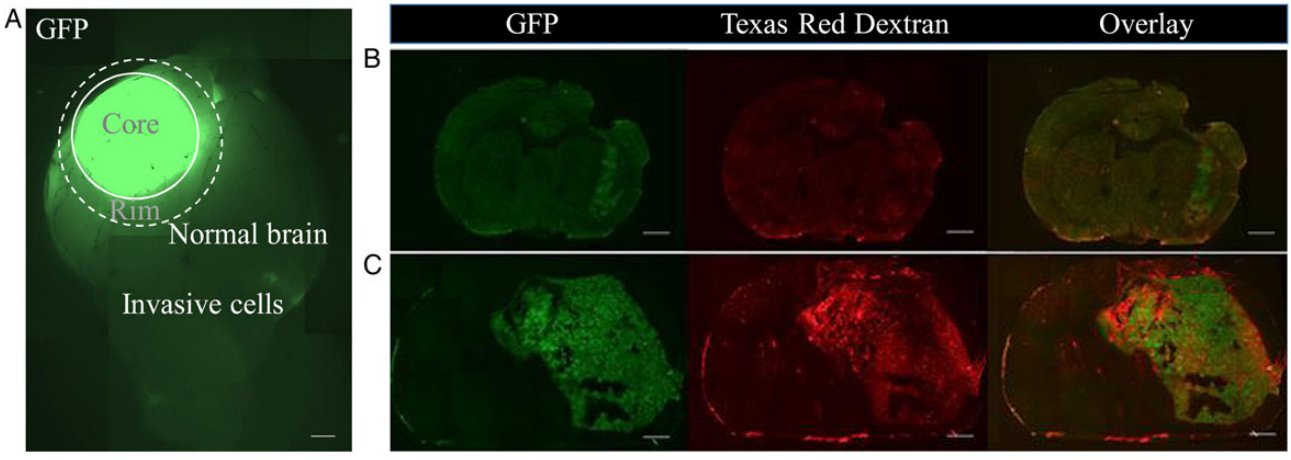

Fig. 2. Characterization of the GL261 murine model. (A) A macroscopic view of GL261-GFP-Luc tumor-bearing brain demonstrates discernible core, rim, and normal brain sections. Scale bar represents 1 mm. (B) and (C) Images of GFP+ tumors and Texas Red dextran infiltration were overlaid to colocalize tumors and heterogeneous BBB disruption. Scale bars represent 1 mm.

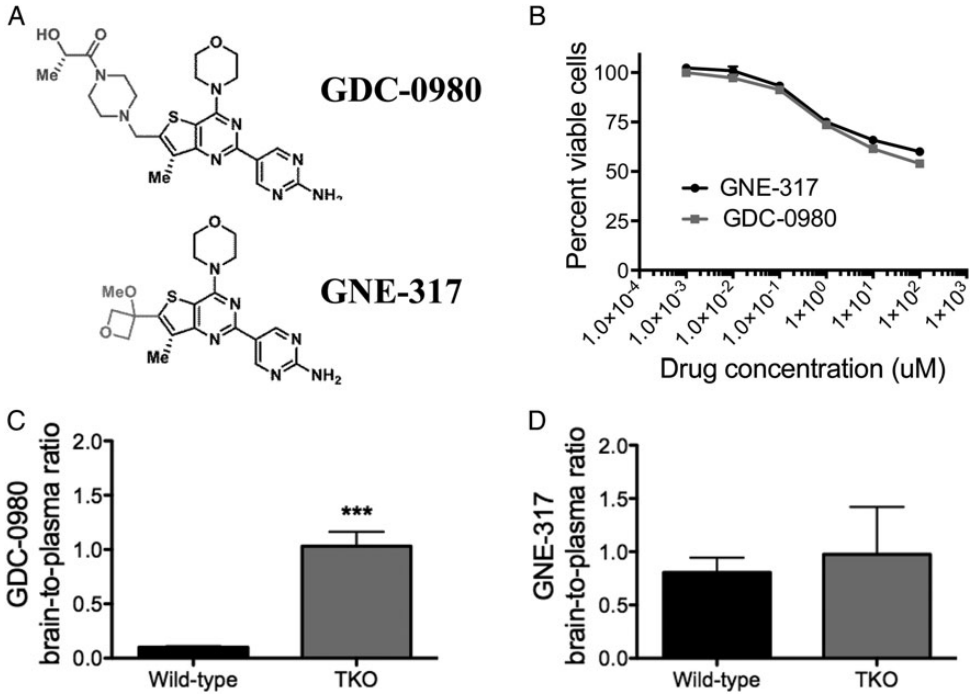

Fig. 3. Cytotoxic and pharmacokinetic comparison of GDC-0980 and GNE-317. (A) Chemicals highlight the common molecular backbone and differentiating side chains. (B) Cytotoxicity of each drug in the GL261 cell line was assessed using the MTS assay. (C) Mdr1/b$^{-/-}$ Bcrp$^{-/-}$ triple knockout (TKO) mice treated with GDC-0980 display a significantly higher ($P < .0005$) brain-to-plasma ratio than wild-type (WT) mice. (D) Mdr1/b$^{-/-}$ Bcrp$^{-/-}$ TKO and WT mice treated with GNE-317 display comparable brain-to-plasma ratios.

acted in a concerted fashion to efflux GDC-0980 (but not GNE-317), and the absence of these transporters in TKO mice resulted in a dramatic enhancement in brain distribution of GDC-0980. Further evaluation of GDC-0980 in PKO and BKO mice showed that P-gp plays a dominant role in restricting brain distribution over BCRP (Supplementary material, Fig. S3).

GNE-317 Penetrates Regions With Invasive Cells More Effectively Than GDC-0980

Brain penetrance of many targeted agents will be expected to differ between regions with a disrupted BBB (eg, the tumor core) and regions with an intact BBB (like the tumor rim). We sought to determine whether drug distribution might also be affected by affinity for P-gp and BCRP in a tumor-bearing animal. C57B6/J mice were intracranially inoculated with GL261-GFP-Luc cells, and tumor growth was tracked through bioluminescence imaging. When tumors reached 5e7 radiance, animals were orally administered the maximum tolerated dose of GDC-0980 (7.5 mg/kg), GNE-317 (30 mg/kg), or vehicle once a day for 3 days. These doses resulted in the same level of total systemic exposure, allowing us to readily compare experimental differences in region-specific brain exposure between treated groups. Mice were euthanized 1 or 6 hours after the final drug administration, and brains were dissected into core, rim, and normal brain as denoted in Fig. 2A and analyzed by LC-MS/MS. Concentrations of GDC-0980 were significantly different between the various regions of the brain. The mean GDC-0980 brain concentration was 720 ± 280 ng/g in the tumor core, 160 ± 100 ng/g in the rim, and 78 ± 37 ng/g in the contralateral hemisphere at 1 hour post last oral dose (Fig. 4A). A similar trend was observed 6 hours after the last drug administration. Concentrations in the tumor core (200 ± 110 ng/g) were higher than those in the rim (40 ± 20 ng/g) and the contralateral hemisphere (70 ± 40 ng/g) (Fig. 4A). Even in the tumor core, the brain-to-plasma ratios demonstrated poor brain penetrance of GDC-0980 (Fig. 4C). In contrast, brain concentrations of GNE-317 were not significantly different in the tumor core, rim, and normal brain (Fig. 4B). The corresponding brain-to-plasma ratios at both 1 hour and 6 hours for the 3 regions of the brain suggested that active efflux by both P-gp and BCRP does not influence brain tumor penetrance of GNE-317 (Fig. 4D). Collectively, these data highlight the importance of substrate affinity for efflux transporters as a key determinant of drug penetrance in various regions of malignant glioma, even in the central tumor mass, where there was an impaired BBB.

GNE-317 Inhibits PI3K/mTOR Pathways More Effectively Than GDC-0980

To determine whether brain penetrance correlates with inhibition of signaling pathways at the tumor and surrounding rim, we used immunohistochemistry to visualize the ability of each drug to inhibit PI3K and mTOR signaling. Tumor-bearing mice were administered 3 doses of drug or vehicle over 3

days once bioluminescence signals reached 5e7 radiance. One hour after the third dose, animals were euthanized, and brains were processed and sliced for staining. Immunohistochemistry focused on downstream targets of the PI3K/mTOR signaling pathway (p-Akt^{Ser473}, p-S6$^{Ser235/236}$, and p-4EBP1$^{Thr37/46}$).[18] Representative stained brain slices are shown in Fig. 5.

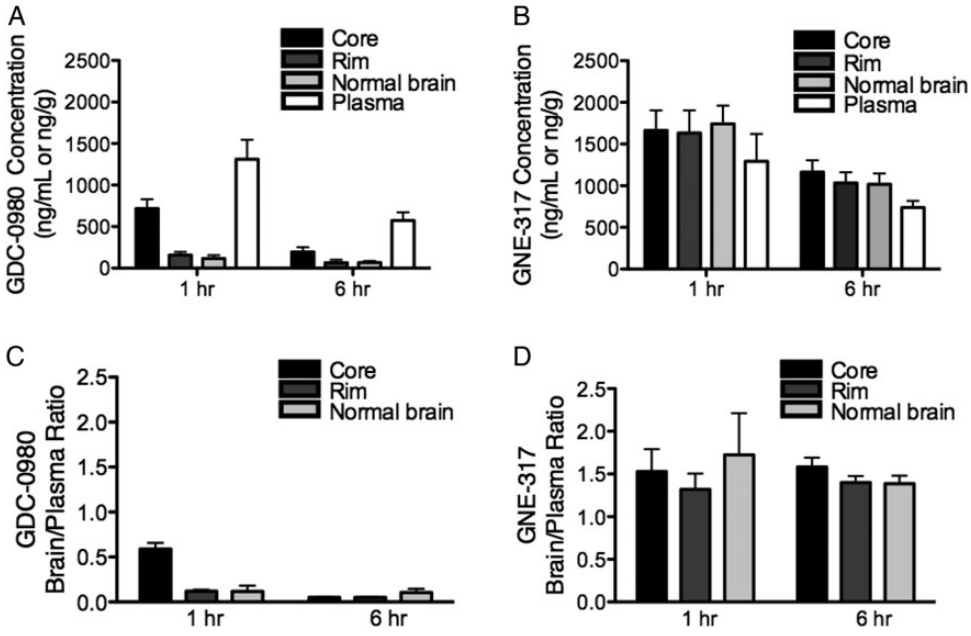

Fig. 4. Regional distribution of GDC-0980 and GNE-317 in a GL261-GFP-Luc tumor-bearing brain. (A) and (C) Regional brain and plasma distributions of GDC-0980 and corroborating brain-to-plasma ratios. (B) and (D) regional brain and plasma distributions of GNE-317 and corroborating brain-to-plasma ratios.

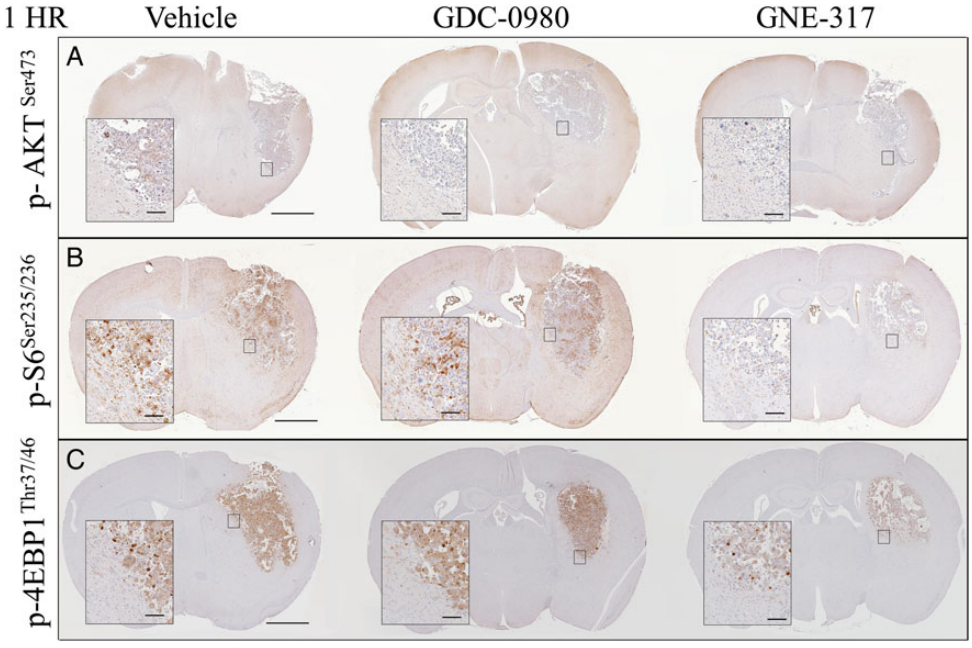

Fig. 5. Immunohistochemistry 1 hour after drug treatment. Scale bars associated with whole slices represent 100 μm, while scale bars associated with close-up insets represent 65 μm. (A) p-Akt^{Ser473} staining is reduced in the presence of GNE-317 and, to a lesser extent, GDC-0980. (B) p-S6$^{Ser235/236}$ staining is reduced in the presence of GNE-317 but not GDC-0980. (C) p-4EBP1$^{Thr37/46}$ staining is reduced in the presence of GNE-317 but not GDC-0980.

Untreated mice showed high-intensity staining of p-S6$^{Ser235/236}$, p-4EBP1$^{Thr37/46}$ and, to a lesser extent, p-Akt^{Ser473} within the tumor (Fig. 5). In particular, p-S6$^{Ser235/236}$ staining was more diffuse within the backgrounds of the brain slices, which was consistent with normal brain mTOR activity. Animals treated with GDC-0980 showed decreased staining for p-Akt^{Ser473} but relatively unchanged staining for p-S6$^{Ser235/236}$ and p-4EBP1$^{Thr37/46}$. In contrast, mice treated with GNE-317 showed substantial reductions in staining intensity within the tumor across all 3 phosphoproteins. Importantly, GNE-317 reduced p-S6 staining not only within the tumor but also in the surrounding normal brain (Fig. 5B). Six hours after dosing, the inhibitory effects of both drugs were largely absent in p-Akt and p-4EBP1 slices, but p-S6 staining was still reduced in mice treated with GNE-317 (Supplementary material, Fig. S4). No differences were seen in staining patterns using nonphosphorylated antibodies (Akt, S6, 4EBP1) 1 or 6 hours after dosing (Supplementary material, Figs S5 and S6), suggesting that overall protein levels remained the same and the changes seen in levels of phosphorproteins between conditions were accurate. These data suggest that differences in substrate affinity for efflux transporters not only impacted brain penetrance (Fig. 4) but also molecular target engagement.

In Vivo Efficacy of GDC-0980 and GNE-317

We next sought to determine how the differences in pharmacokinetics and pharmacodynamics observed between GDC-0980 and GNE-317 would impact tumor growth and survival. Seven days after i.c. inoculation with GL261-GFP-Luc cells, mice were treated once daily with the maximum tolerated dose of GDC-0980 (7.5 mg/kg), GNE-317 (30 mg/kg), or vehicle. For GL261, tumor growth was tracked through bioluminescence imaging on a weekly basis (Fig. 6A). There were no significant changes in GL261 tumor growth among the 3 groups. In assessing survival benefits in GL261, neither GDC-0980 nor GNE-317 provided survival benefit over the vehicle-treated animals (Fig. 6B). The fact that these drugs were not effective in vivo is suggested by the in vitro cytotoxicity data showing that the drugs have limited efficacy in inducing cell death in the GL261 cell line (Fig. 3B). Neither drug was effective in the GL261 tumor in spite of greater delivery and enhanced therapeutic targeting efficacy of GNE-317.

Discussion

The results of this study demonstrate the impact that affinity for efflux transporters can have on chemotherapeutic brain penetrance and molecular target engagement. We first demonstrated that the GL261 mouse model is an accurate representation of these qualities compared with human GBM pathology (Fig. 2). By experimenting with 2 PI3K/mTOR analogues that possess the same molecular backbone and targeting capacity,[16] and similar physicochemical properties (Supplementary material, Fig. S7), we directly measured the influence of efflux transporter substrate affinity in the treatment of GBM. Drug distribution studies in non–tumor- and tumor-bearing mice indicated that GNE-317 has better brain penetrance than GDC-0980 because the distribution of GNE-317 is not limited by active efflux at the BBB (Figs 3 and 4). We also determined that brain penetrance positively correlates with efficacy in molecular targeting, with GNE-317 being more efficacious than GDC-0980 at downregulating the PI3K and mTOR pathways (Fig. 5).

Despite the impact these drugs have on inhibition of PI3K/mTOR signaling, there were no demonstrable changes in tumor growth or survival (Fig. 6). These data reinforce another important issue in drug design for GBM target selection. The inability of these drugs to provide survival benefits is likely specific to the GL261 model, as other glioma models have been shown to be sensitive to these agents.[27] Previous work in conjunction with our in vitro data (Fig. 3B) demonstrated that GL261 is at least partially driven by PI3K signaling,[19] but other pathways likely play parallel roles in tumor growth and development,[28] and combination therapies may be warranted. This failure does not preclude GDC-0980 or more likely, GNE-317, from being more successful in other models or in patients whose gliomas are primarily driven by these other pathways. The increase in brain penetrance and ability to effectively inhibit PI3K/mTOR pathways in our study still confirms that GNE-317 is capable of on-target effects in vivo and points to the fact that all drugs in the combination should be brain penetrant if combination targeted therapy is used for invasive brain tumors.

The current study measuring brain penetrance and target inhibition in both tumor and normal brain provides data that are difficult to obtain in human patients. While clinicians have the ability to measure drug concentration in the homogenized

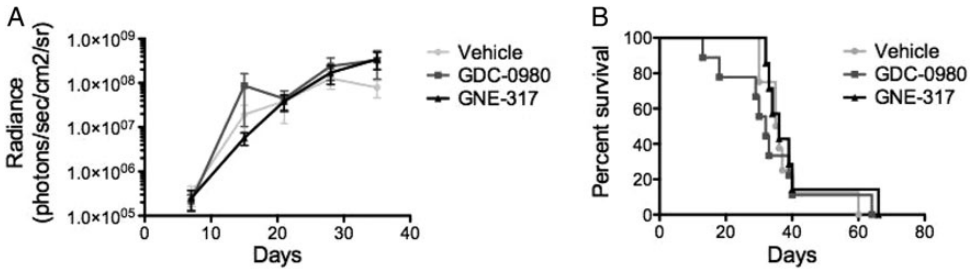

Fig. 6. In vivo efficacy studies. (A) Tumor progression tracked through bioluminescent imaging shows no demonstrable impact of either GDC-0980 or GNE-317 over vehicle-treated animals. (B) Kaplan-Meier survival curve indicates that neither GDC-0980 nor GNE-317 provides survival benefit over vehicle.

tumor core following surgical resection, data from surrounding brain with invasive tumor cells are more difficult to obtain. Unfortunately, drug concentration data from the tumor core where the BBB is heterogeneously disrupted do not accurately reflect drug concentrations in other areas of the brain. The lack of biomarkers or imaging techniques capable of indicating successes or failures in drug delivery therefore necessitates that clinicians understand the potential brain penetrance of a drug before its clinical application. This knowledge will help clinicians introduce chemotherapies into clinical trials that have a better chance of success.

The importance of brain penetrance of chemotherapeutics has significant implications for the development and evaluation of novel drugs for GBM. Recent attempts to determine drug concentrations and pharmacodynamic responses in tumor and normal brain samples from human patients[29] highlight the importance of chemotherapeutic brain penetrance. By eliminating drug delivery issues as a variable in the failures of clinical trials, therapeutic target selection can receive greater attention and consideration. In simplest terms, if we can be assured of adequate delivery, we can then choose drugs based on information about tumor heterogeneity that would not be confounded by differences in delivery.

This study also draws attention to the process of drug discovery and development. Brain-penetrant chemotherapies can be re-designed from existing chemotherapeutics that have a high substrate affinity for efflux transporters. As elegantly illustrated by Heffron et al[16] and Salphati et al[27], a drug with limited brain penetration can be used as a scaffold to develop highly brain-penetrant analogues with a greater potential for clinical efficacy. At a time when the cost of creating a new drug surpasses US$5 billion[30] the ability to modify existing compounds into new agents with potentially drastic changes in targeted bioavailability to sites of action cannot be undervalued.

Supplementary Material

Supplementary material is available online at *Neuro-Oncology* (http://neuro-oncology.oxfordjournals.org/).

Funding

National Institute of Neurological Disease and Stroke (NS077921 to W.E. and J.S.); National Cancer Institute (CA138437 to W.E. and J.O.); Children's Cancer Research Foundation (to D.L.)

Conflict of interest statement. J.N. Sarkaria: research funding from Genentech, Inc.; D.A. Largaespada: co-founder and part owner of Discovery Genomics, Inc (DGI); Genentech, Inc. grant recipient; W.F. Elmquist: consulting relationship with Genentech, Inc.

References

1. Grossman SA, Ye X, Piantadosi S, et al. Survival of patients with newly diagnosed glioblastoma treated with radiation and temozolomide in research studies in the united states. *Clin Cancer Res*. 2010;16(8):2443–2449.
2. Wilson TA, Karajannis MA, Harter DH. Glioblastoma multiforme: State of the art and future therapeutics. *Surg Neurol Int* 2014;5:64. 7806.132138. eCollection 2014.
3. Haar CP, Hebbar P, Wallace GC, et al. Drug resistance in glioblastoma: A mini review. *Neurochem Res*. 2012;37(6):1192–1200.
4. Pafundi DH, Laack NN, Youland RS, et al. Biopsy validation of 18F-DOPA PET and biodistribution in gliomas for neurosurgical planning and radiotherapy target delineation: Results of a prospective pilot study. *Neuro Oncol*. 2013;15(8):1058–1067.
5. Karunanithi S, Sharma P, Kumar A, et al. Comparative diagnostic accuracy of contrast-enhanced MRI and (18)F-FDOPA PET-CT in recurrent glioma. *Eur Radiol*. 2013;23(9):2628–2635.
6. Deeken JF, Loscher W. The blood-brain barrier and cancer: transporters, treatment, and Trojan horses. *Clin Cancer Res* 2007;13(6):1663–1674.
7. Abbott NJ, Rönnbäck L, Hansson E. Astrocyte–endothelial interactions at the blood–brain barrier. *Nat Rev Neurosci*. 2006;7(1):41–53.
8. Agarwal S, Sane R, Oberoi R, et al. Delivery of molecularly targeted therapy to malignant glioma, a disease of the whole brain. *Expert Rev Mol Med*. 2011;13:e17.
9. Agarwal S, Hartz AM, Elmquist WF, et al. Breast cancer resistance protein and P-glycoprotein in brain cancer: two gatekeepers team up. *Curr Pharm Des* 2011;17(26):2793–2802.
10. Robey RW, Massey PR, Amiri-Kordestani L, et al. ABC transporters: unvalidated therapeutic targets in cancer and the CNS. *Anticancer Agents Med Chem*. 2010;10(8):625–633.
11. Krishna R, Mayer LD. Multidrug resistance (MDR) in cancer: Mechanisms, reversal using modulators of MDR and the role of MDR modulators in influencing the pharmacokinetics of anticancer drugs. *Eur J Pharm Sci*. 2000;11(4):265–283.
12. Gabathuler R. Approaches to transport therapeutic drugs across the blood-brain barrier to treat brain diseases. *Neurobiol Dis*. 2010;37(1):48–57.
13. Pardridge WM. Blood-brain barrier delivery. *Drug Discov Today*. 2007;12(1):54–61.
14. Levatic J, Curak J, Kralj M, et al. Accurate models for P-gp drug recognition induced from a cancer cell line cytotoxicity screen. *J Med Chem*. 2013;56(14):5691–5708.
15. Berens ME, Giese A. "... Those left behind." Biology and oncology of invasive glioma cells. *Neoplasia*. 1999;1(3):208–219.
16. Heffron TP, Salphati L, Alicke B, et al. The design and identification of brain penetrant inhibitors of phosphoinositide 3-kinase alpha. *J Med Chem*. 2012;55(18):8007–8020.
17. Cancer Genome Atlas Research Network. Comprehensive genomic characterization defines human glioblastoma genes and core pathways. *Nature*. 2008;455(7216):1061–1068.
18. Sami A, Karsy M. Targeting the PI3K/AKT/mTOR signaling pathway in glioblastoma: Novel therapeutic agents and advances in understanding. *Tumour Biol*. 2013;34(4):1991–2002.
19. Newcomb EW, Zagzag D. *The murine GL261 glioma experimental model to assess novel brain tumor treatments*. In: Van Meir EG, ed. *Cancer. Models, Markers, Prognostic Factors, Targets, and Therapeutic Approaches*. New York, NY: New York University School of Medicine; 2009:227–241.
20. Wu A, Oh S, Ericson K, et al. Transposon-based interferon gamma gene transfer overcomes limitations of episomal plasmid for immunogene therapy of glioblastoma. *Cancer Gene Ther*. 2007;14(6):550–560.

21. Wu A, Oh S, Gharagozlou S, et al. In vivo vaccination with tumor cell lysate plus CpG oligodeoxynucleotides eradicates murine glioblastoma. *J Immunother*. 2007;30(8):789–797.
22. Ohlfest JR, Demorest ZL, Motooka Y, et al. Combinatorial antiangiogenic gene therapy by nonviral gene transfer using the sleeping beauty transposon causes tumor regression and improves survival in mice bearing intracranial human glioblastoma. *Mol Ther* 2005;12(5):778–788.
23. Agarwal S, Mittapalli RK, Zellmer DM, et al. Active efflux of dasatinib from the brain limits efficacy against murine glioblastoma: broad implications for the clinical use of molecularly targeted agents. *Mol Cancer Ther*. 2012;11(10):2183–2192.
24. Oberoi RK, Mittapalli RK, Elmquist WF. Pharmacokinetic assessment of efflux transport in sunitinib distribution to the brain. *J* Pharmacol Exp Ther. 2013;347(3):755–764.
25. Dai H, Marbach P, Lemaire M, et al. Distribution of STI-571 to the brain is limited by P-glycoprotein-mediated efflux. *J Pharmacol Exp Ther*. 2003;304(3):1085–1092.
26. Leten C, Struys T, Dresselaers T, et al. In vivo and ex vivo assessment of the blood brain barrier integrity in different glioblastoma animal models. *J Neurooncol*. 2014;119(2):297–306.
27. Salphati L, Heffron TP, Alicke B, et al. Targeting the PI3K pathway in the brain--efficacy of a PI3K inhibitor optimized to cross the blood-brain barrier. *Clin Cancer Res*. 2012;18(22):6239–6248.
28. Szatmari T, Lumniczky K, Desaknai S, et al. Detailed characterization of the mouse glioma 261 tumor model for experimental glioblastoma therapy. *Cancer Sci*. 2006;97(6):546–553.
29. Pitz MW, Desai A, Grossman SA, et al. Tissue concentration of systemically administered antineoplastic agents in human brain tumors. *J Neurooncol*. 2011;104(3):629–638.
30. Herper M. *The Cost Of Creating A New Drug Now $5 Billion, Pushing Big Pharma To Change. Forbes*. August 11, 2013. http://www.forbes.com/sites/matthewherper/2013/08/11/how-the-staggering-cost-of-inventing-new-drugs-is-shaping-the-future-of-medicine. Accessed September 1, 2014.